Title

On the capillary pressure function in porous media based on relative permeabilities of two immiscible fluids: Application of capillary bundle models and validation using experimental data

Authors

Babchin, AJ

Bentsen, R

Faybishenko, B

et al.

Publication Date

2016-07-01

DOI

10.1016/j.cis.2015.07.001

Peer reviewed

On the capillary pressure function in porous media based on relative permeabilities of two immiscible fluids: Application of capillary bundle models and validation using experimental data

Author links open overlay panelA.J.Babchin[ab]R.Bentsen[c]B.Faybishenko[d]M.B.Geilikman[e]
Show more

https://doi.org/10.1016/j.cis.2015.07.001Get rights and content

Abstract

The objective of the current paper is to extend the theoretical approach and an analytical solution, which was proposed by Babchin and Faybishenko (2014), for the evaluation of a capillary pressure (P_c) curve in porous media based on the apparent specific surface area, using an explicit combination of the relative permeability functions for the wetting and nonwetting phases. Specifically, in the current paper, the authors extended this approach by the application of two types of capillary bundle models with different formulations of effective capillary radius formulae. The application of the new models allowed the authors to improve the results of calculations of the effective average contact angle given in the paper by Babchin and Faybishenko (2014). The validation of the new models for calculations of the P_c curve is also given in this paper using the results of a specifically designed core experiment, which was originally conducted by Ayub and Bentsen (2001).

Graphical abstract

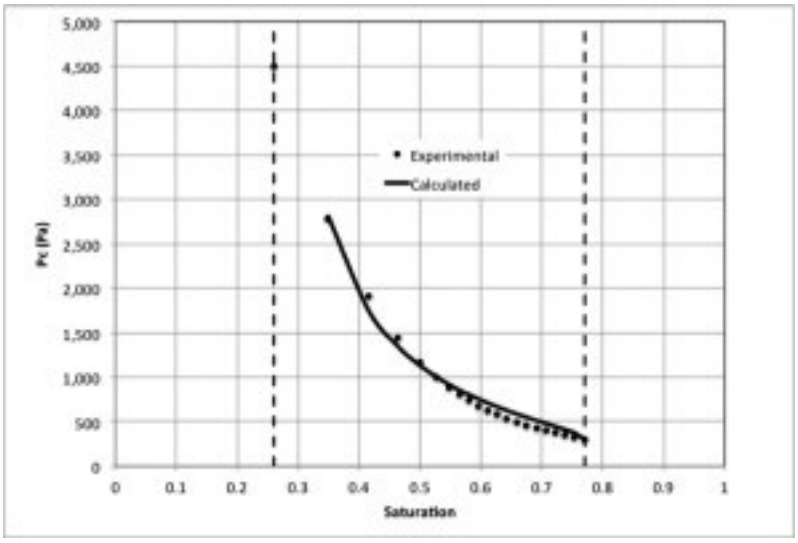

1. Download high-res image (53KB)
2. Download full-size image

Keywords

Capillary pressure curve
Relative permeability functions
Wetting and nonwetting phases
Capillary bundle models

1. Introduction

Despite many decades of investigations of two-phase (wetting and nonwetting) transport phenomena in porous media, there are fundamental problems with the application of differential equations for modeling because of the nature and choice of appropriate relationships for the two relative permeabilities and capillary pressure as functions of saturation. Moreover, it is not clear how these functions should be determined using experiments [1], [2].

In their recent paper, Babchin and Faybishenko [3] proposed to determine first an apparent specific surface area of porous media, using an explicit combination of the relative permeability functions for the wetting and nonwetting phases, and then used the combination to determine the capillary pressure-saturation function. The application of this approach was demonstrated for the drainage and imbibitioncapillary pressure curves using published experimental data from [4], [5], [6]. The results of calculations in [3] confirmed that the use of a single effective average contact angle, Θ, is not a physically correct approach for systems where there is a distribution of contact angles, especially in the event of fractional wettability, nonwetting-phase entrapment, and redistribution of the nonwetting phase between different types of pores [7], [8], [9], [10].

In the current paper, the authors extended the theoretical background of the idea of the evaluation of the capillary pressure function based on the apparent specific surface area of porous media, revised the results of the calculations presented in [3], as well as presented a set of new calculations based on the experimental data coauthored by one of the coauthors of this paper [11], [12].

2. Basic capillary models

2.1. Effective hydraulic radius models

Modeling of flow through the interparticle interstices of real porous media is often based on the concept of presenting porous media as a bundle of capillary columns/tubes. This concept has proved to be very useful for studies of flow and transport in hydrological and technological studies [13], [14]. Because irregular-shaped interstitial pores are not straight cylinders, the porous space has to be modeled using an

effective hydraulic radius. Several approaches have been proposed for the assessment of the effective hydraulic radius [15], [16], [17]. In this paper, we will consider the following three approaches:

1. The hydraulic radius
2. The radius of an equivalent capillary
3. The real internal or intrinsic scale, that is, the pore size or radius of the capillary

1. *The hydraulic radius.* The hydraulic radius is defined as the radius of a straight capillary of constant cross section, and it can be calculated using its volume, V, and surface area, S, as follows:

(1) $$rH=2VS\equiv 2Sv$$

where the specific surface is determined as the surface area per unit volume:

(2) $$Sv=SV$$

The definition of hydraulic radius given by Eq. (1) can be applied to the entire porous medium, which will be discussed below in this paper.

2. *The radius of an equivalent capillary.* The radius of an equivalent capillary, r, is calculated based on the following formula for the flow rate [16]:

(3) $$Q=-\pi r48\mu gradP$$

where μ is the viscosity. From Eq. (3), for a unit area, the total flow through the equivalent capillaries is given by

(4) $$q=Q\pi r2=-r28\mu gradP$$

For the same unit area, Darcy flow is expressed as follows:

(5) $$q=-K\mu gradP$$

where K is the absolute permeability.

By equating q, given by Eqs. (4), (5), one can obtain the following expression for the equivalent cylindrical capillary in terms of the absolute permeability, K, of the porous medium:

(6) $$r=8K$$

The expression given by Eq. (6) can be called the “radius of an equivalent capillary” for a porous medium with permeability K. Note that Eq. (6)includes only

the dependence of the *equivalent radius of porous media* on permeability, which is different from Leverett's expression for the dependence of *r* on *K* and porosity, as well as other expressions of the dependence of r on the pore size distribution.

3. *The real internal or intrinsic scale.* This is a real scale in a porous medium such as the pore size or the radius of the capillary (see Fig. 1, Fig. 2), which is a bottleneck in transport in porous media theory.

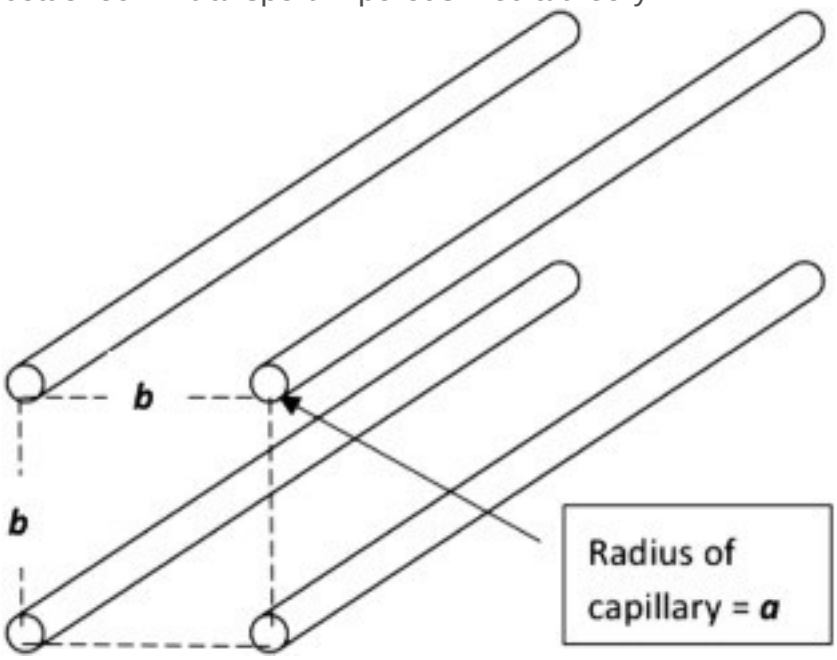

1. Download high-res image (72KB)
2. Download full-size image

Fig. 1. Schematic of a porous medium model as a bundle of parallel capillaries.

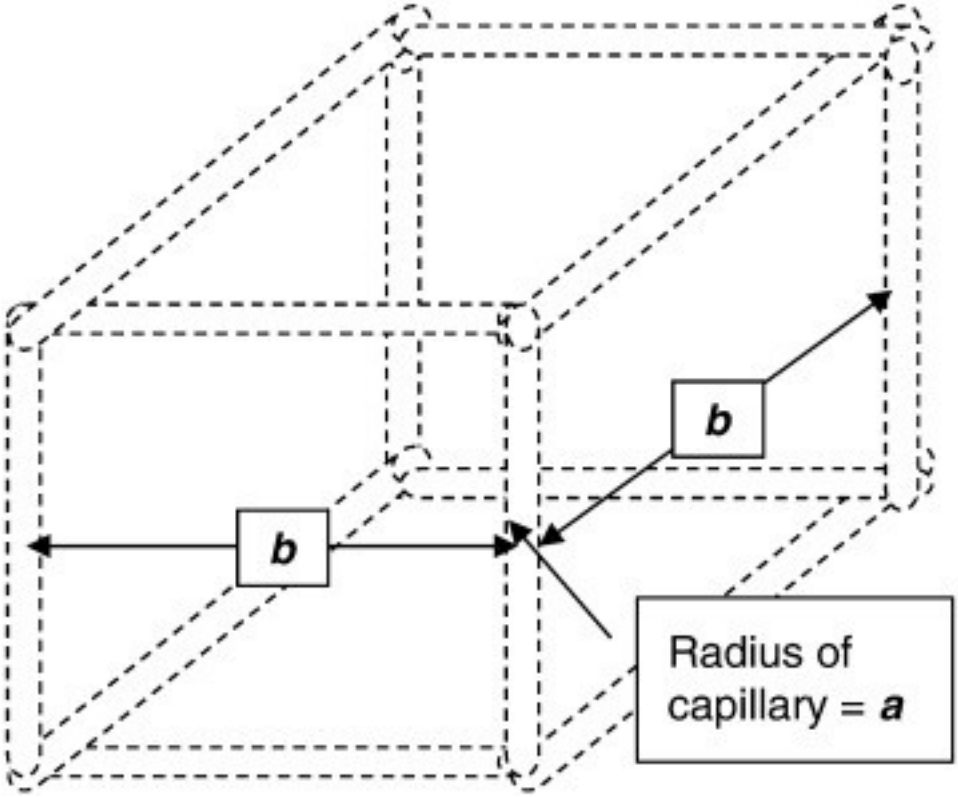

1. Download high-res image (177KB)
2. Download full-size image

Fig. 2. Schematic of a model of porous medium as two perpendicular intersecting bundles of parallel capillaries.

2.2. Model of a porous medium as a bundle of parallel capillaries

The capillary tube models are often used to describe both the permeability and the capillary pressure function, which are primary characteristic parameters of porous media. Despite the long history of using capillary tube models, starting from the classical Kozeny–Carman equation that was derived for a medium represented by pipe conduits, several alternative formulations have been proposed recently to improve the use of these models (e.g., [34], [35], [36], [37], [38], [39]). In their recent review of the conceptual models of porous media, Hunt et al. [40] indicated the capillary tube bundle model “represents the medium as a collection of right circular cylinders, all of the same length, and occurring with a frequency that gives the same volume pdf as the medium.” The same authors stated that “[a]ditional physics may be added in the form of misalignment of tubes to create tortuosity, variable tube radii to generate the inkbottle effect, etc.”

Fig. 1 depicts a schematic of a porous medium model consisting of a bundle of cylindrical capillaries, as assumed by Leverett in his modeling of porous media. In this model, the porosity is given by the following expression:

(7)$$\phi = \pi a^2 b^2$$

where a is the radius of the cylindrical capillaries and b is the spacing between them (see Fig. 1). The specific surface for this model is given by

(8)$$S_v = 2\pi a b^2$$

The permeability of the model of parallel capillaries is expressed as follows:

(9)$$K = \frac{\pi a^4}{8 b^2}$$

By using Eqs. (7), (8), we can eliminate the geometric parameters from the equation for permeability (9). As a result, we obtain for the permeability:

(10)$$K = \frac{\phi^3}{2 S_v^2}$$

Expression (10) resembles the well-known Carman–Kozeny formula, which relates the permeability and the specific surface (e.g., [14]).

Substitution of Eq. (10) into Eq. (6) gives rise to the following relationship between the equivalent capillary radius, porosity, and specific surface:

(11)$$r = \frac{8K}{2\phi^3} = \frac{2}{S_v}$$

whereas the hydraulic radius defined by Eq. (1) is determined, after using Eq. (10), through the porosity and permeability as follows:

(12)$$r_H = \frac{2}{S_v} = \frac{2\phi^3}{2K}$$

By using the equation for porosity (Eq. (7)), we can eliminate the spacing parameter b from Eq. (9) for permeability, while keeping the radius of the capillary a. As a result, we obtain an expression for the radius of the capillary, which is defined in terms of the macroscopic characteristics of the porous medium—porosity and permeability:

(13)$$a = \frac{8K}{\phi}$$

The term $(K/\phi)^{1/2}$ in Eq. (13) is called the characteristic length of the porous medium or the “radius of an equivalent capillary” [4], [16]. Following Barenblatt et al. [14], we will call it the “internal or intrinsic length.”

2.3. Model of a bundle of orthogonal capillaries

Now let’s consider a more complicated model of a porous medium, consisting of a set of orthogonal intersecting bundles of parallel capillaries (Fig. 2). Using the aforementioned approach for the model of a single bundle of parallel capillaries, we obtain the equations for the porosity:

(14)$$\phi = 3\pi a^2 b^2$$

the specific surface:

(15)Sv=6πab2

and the permeability:

(16)K=πa48b2

Again, using Eqs. (14), (15), we can eliminate the geometric parameters *a* and *b*from the equation for permeability (16), and, as a result, we obtain for the permeability of the model of a set of orthogonal bundles of parallel capillaries:

(17)K=ϕ36Sv2

The structure of Eq. (17) is similar to that of the Carman–Kozeny formula, but with a different numerical coefficient as compared to Eq. (10) obtained for the permeability in the model of a single bundle of parallel capillaries.

For the equivalent capillary radius, we obtain from Eqs. (6), (17):

(18)r=8K=23·ϕ3/2Sv

The expressions for the equivalent capillary radius and the hydraulic radius differ from those for the previous model (see Eqs. (11), (12)) only in the numerical coefficients:

(19)rH=2Sv=2ϕ3/23K

According to Eq. (6), the radius of an equivalent capillary, *r*, is expressed through the macroscopic characteristic permeability. The radius of an equivalent capillary, *r*, relates to the radius of the capillary, *a*, for the models of single and orthogonal bundles of capillaries, through Eqs. (6), (7), (9), (14), (16):

(20)r=8K=aϕ·1;forasinglebundleofcapillaries13;fororthogonalbundlesofcapillaries

Let’s also express the hydraulic radius through the macroscopic characteristics of the porous medium, the permeability, and the porosity. Using Eq. (1) for hydraulic radius and the equations for permeability (Eqs. (10), (19)), we arrive at the following expression:

(21)rH=Kϕ3·22;forasinglebundleofcapillaries26;fororthogonalbundlesofcapillaries

Finally, let’s express the internal scale, that is, the real radius of the capillary via porosity and permeability, not only for the model of a single bundle of capillaries as given by Eq. (13) but also for the model of capillary bundles:

(22)a=Kϕ·22forasinglebundleofcapillaries26fororthogonalbundlesofcapillaries

As can be seen from Eqs. (20), (21), (22), all three basic lengths of porous media, defined above, are proportional to the square root of permeability, which is obvious from dimensional analysis. However, these three characteristic lengths depend differently on porosity.

It should be noted that both of the specific capillary models described above lead to Carman–Kozeny-type of expressions for permeability $K \sim \phi^3/S_v^2$. The Carman–Kozeny expression, being probably the most widely used and recognized, is not the only one

possible among various permeability models (see, e.g., Dullien, 1992). We could hypothesize that for those models (which do not exhibit Carman–Kozeny behavior), a characteristic scale of the porous medium, l, is determined as follows:

(23)$$l = f\phi K$$

where $f(\phi)$ is a dimensionless, model-dependent function of porosity.

3. Calculations of the capillary pressure function

Numerical simulations of transport phenomena of two immiscible fluids, such as NAPL and water, in porous media are usually based on Darcy's law given for each phase by

$$q_n = -KK_{rn}\mu_n \text{grad} P_n$$

$$q_w = -KK_{rw}\mu_w \text{grad} P_w$$

where q_n and q_w are the volumetric flow rates of the nonwetting and wetting phases, respectively, through a unit area, normal to the flow; K is the porousmedium absolute permeability; K_{rn} and K_{rw} are the relative permeabilities of the nonwetting and wetting phases, respectively; μ_n and μ_w are the viscosities of the nonwetting and wetting phases, respectively; P_n and P_w are the pressures of the nonwetting and wetting phases, respectively; and the capillary pressure is given by $P_c = P_n - P_w$.

For the purposes of the simulation of the flow of two immiscible fluids, P_c is often expressed by means of the Leverett J function [16]. Burdine [17] introduced a tortuosity factor in his model describing the relationship between relative permeability and capillary pressure, which for the case of two-phase flow is given by

(24)$$K_{rw} = \lambda_w 2\int_0^{Sw} \frac{dSw}{Pc^2} \Big/ \int_0^1 \frac{dSw}{Pc^2} \qquad K_{rn} = \lambda_n 2\int_{Sw}^1 \frac{dSn}{Pc^2} \Big/ \int_0^1 \frac{dSn}{Pc^2}$$

where λ_w and λ_n are tortuosity factors, and where the symbols w and n denote the wetting and nonwetting phases, respectively, and S_w and S_n are the saturations of the wetting and nonwetting phases, respectively. However, the tortuosity factors are not explicitly defined and cannot be measured; thus, they are just fitting parameters.

Rapoport and Leas [18] were probably the first to suggest that the capillary pressure (P_c) and relative permeability functions are dependent on interfacial area (although they have been modeled typically as functions of fluid saturation). In the past 20–25 years, various numerical models and modeling techniques have been developed to simulate subsurface multiphase flow at the pore scale, including pore network models and Lattice–Boltzmann models [19], [20], [21], [22]. An application of a thermodynamically constrained macroscale description of flow in porous media, which explicitly takes into account the presence of interfaces, was proposed in [23], [24]. However, despite the wide interest in measuring and calculating specific interfacial area and capillary pressure, there are surprisingly few works on this subject [25]. Using interfacial area

requires conducting experiments at the microscopic scale, whereas using saturation requires experiments at the macroscale.

Contrary to single-phase flow, where the specific surface area averaged over the total volume of a core sample is a constant value, in the case of two-phase flow of immiscible fluids, the total specific surface area is a function of the phase distributions, and the total specific surface area is the sum of the phase specific surface areas. The wetting phase tends to reside in the smaller pores, while the nonwetting fluid resides in the larger pores. At residual wetting and nonwetting saturations, the specific surface values asymptotically approach infinity. Indeed, the residual wetting phase is located in the smallest capillaries, as tiny ganglia, or as pendular drops, bridging the solid grains. All of these configurations have very small radii and, hence, high capillary pressure. Consequently, they exhibit high capillary resistance to flow, which the pressure gradient, imposed by displacement fluid flow, is incapable of overcoming. Complete immobilization of the residual fluid is either equivalent to the apparent radii approaching a value of zero, or to the magnitude of the specific surface approaching infinity. In other words, capillarity effects should be taken into account in the evaluation of the specific surface area for a two-phase flow system in porous media, as these effects induce additional resistance to flow. Even in a simplified droplet train model, capillary forces are capable of inducing additional resistance to flow [26].

Babchin and Nasr [27] derived a simplified analytical expression for the capillary pressure gradient in homogeneous, porous two-fluid media, containing three bulk phases (solid phase, wetting, and nonwetting fluids), with three possible interfaces (solid–wetting, solid–nonwetting, and nonwetting–wetting). They assumed a finite value of the three-phase contact angle among the two fluids and a solid phase of porous rock, and that the contact surface area between two continuous fluid phases is small in comparison with the contact surface areas between each fluid and the porous rock in a unit volume of the rock. The surface energy of such a system is given by

(25)W=γn−s.Sv.Sn+γw−s.Sv.Sw+γn−wσn−w,

where W is the density of the excess energy of the porous medium associated with the interfaces. In other words, it is the additional density of the surface energy due to the presence of two fluids within a porous rock. Also, S_v is the specific surface area of the porous medium; γ_{n-s}, γ_{w-s}, and γ_{n-w} are the nonwetting phase–solid, wetting phase–solid, and nonwetting–wetting phases specific surface energies, respectively; S_n and S_w are the saturations of the nonwetting liquid and water, subject to $S_n + S_w = 1$; and σ_{n-w} is the area of the nonwetting–wetting phase interface within a unit volume of porous medium.

According to [27], the area of direct contact between two immiscible fluids in a one-Darcy permeability porous medium is five orders of magnitude smaller than the area of contact between these fluids and the solid grains; therefore, the last term of Eq. (25) can be neglected. (For solid–liquid and liquid–liquid contact areas to be of the same order of magnitude, one fluid would have to be emulsified in the other, and the droplet size would have to be of the same order of magnitude as the solid grain size. Such a state is known as emulsion flow, where one of the fluids is in a discontinuous state, and no three-phase contact angle exists. This kind of flow is rarely observed and is outside the scope of this paper.)

Eq. (25) is then given by

(26)$$W \approx \gamma_{n-s} - \gamma_{w-s}.S_v.S_n + \gamma_{w-s}.S_v$$

By using the standard Young equation, $\gamma_{n-s} - \gamma_{w-s} = \gamma_{n-w} \cos \Theta$, where Θ is the wetting-phase contact angle, we can express W as

(27)$$W \approx \gamma_{n-w}.\cos\Theta.S_v.S_n + \gamma_{w-s}.S_v$$

When $S_w = 1$, the second term in Eq. (27) corresponds to the condition of full water saturation of the pore space. The first term of Eq. (27) represents the energy arising from the capillary pressure, which is developed in a system of two immiscible fluids in porous media.

(28)$$P_c \approx \gamma_{n-w}.\cos\Theta.S_v.S_n$$

The value of S_v in Eq. (28) can be expressed as an averaged value for a volume V of porous medium in the following integral form:

(29)$$S_v = \frac{1}{V}\int_v \bar{S_v} dV$$

The value of $\bar{S_v}$ in Eq. (29) can be specified as the sum of two components—one for the nonwetting phase, the other for the wetting phase, both being saturation dependent. For the case of a single fluid residing in a porous medium, the averaged value of the specific surface area Sv can be expressed using the Carmen–Kozeny formula, Eq. (10), as

(30)$$S_v = \phi^{3/2} K^{0.5}$$

In the case of the transport of two immiscible fluids in a porous medium, the permeabilities of the nonwetting and wetting phases, subject to $S_{nw} + S_w = 1$, can be expressed in terms of their relative permeabilities, which are functions of the phase saturations, given by

(31a)$$K_{nw} = K K_{rn} S_{nw}$$

(31b)$$K_w = K K_{rw} S_w$$

By substituting Eqs. (31a), (31b) into Eq. (30), one can define the specific surfaces separately for the nonwetting and wetting phases as

(32a)Svn=ϕ3/2KKrn0.5

(32b)Svw=ϕ3/2KKrw0.5

The relative permeability of each phase is a carrier of information about the averaged value of the specific surface of the porous medium, where this phase resides, so we can express the averaged value of the specific surface (see Eq. (29)), as the sum of the specific surfaces of both phases:

(33)Sv=ϕ3/2K0.51/Krn0.5+1/Krw0.5

For the case of the bundle of capillaries model, the specific surface equation differs from Eq. (33) in the constant coefficient only, and the term including the relative permeabilities remains the same. Thus,

(34)Svb=ϕ3/6K0.51/Krn0.5+1/Krw0.5

A comparison of both Eqs. (33), (34) with available experimental data will be presented in Section 5 of this paper.

Because, at the residual saturation points S_{rn} and S_{rw}, for the nonwetting and wetting phases, respectfully, $K_{rn} = 0$ and $K_{rw} = 0$, Eqs. (33), (34) become singular, i.e., the function is neither finite nor differentiable. The singularity at $K_{rw} = 0$ (at $s = s_{rw}$) corresponds to the well-known phenomenon of an infinite suction pressure at the irreducible wetting-phase saturation [28]. The physical explanation of these phenomena is as follows: at the residual saturation points, the fluid phase resides in tiny pores or in the form of bridges matching the grains or tiny ganglia, all of which have a very small radius, resulting in very high capillary pressures, which resist either the displacement or the imbibition process beyond the residual saturation points. For example, the residual oil saturation is defined, generally, as the oil content that remains in an oil reservoir at depletion, when oil ceases to be recovered [29]. The residual oil saturation in the reservoir can range from 2% to 50%, with an approximate average value ranging from 15% to 20% [30]. Note that the results of laboratory and field tests are often inconsistent and lead to uncertainty in the values of the oil residual saturation [31].

To remove the infinite values from the calculations, we can employ a system of reduced (normalized) saturations s_n and s_w for the nonwetting and wetting phases, respectively, given by [11]

(35a)sn=Sn–Srn/1–Srn–Srw

(35b)sw=Sw−Srw/1−Srn−Srw

By expressing the nonwetting-phase saturation in a reduced (normalized) form, we finally come to the following expression for the nonwetting phase–water–solids capillary pressure:

(36)Pc=γnwcosθ.Sv.sn+A

where S_v is given by either Eq. (33) or Eq.(34), s_n is given by Eq. (35a), A is a constant that corresponds to the initial displacement pressure, when the wetting phase is displaced by the nonwetting phase, and $A = 0$ for imbibition [11]. Based on Eq. (36), the intrinsic hysteresis of P_c for drainage (water is displaced by nonwetting phase) and imbibition (nonwetting phase is displaced by water) conditions is determined by the constant A.

Thus, the functional dependence of P_c is given in terms of the relative permeabilities of wetting and nonwetting phases. The relative permeabilities implicitly take into account the geometry (topology), as well as the roughness and crevices of the porous medium. By using relative permeability functions, we automatically obtain singularities at the residual points, which are universally accepted. It will be shown in Section 5 of the paper that using corrected coefficients of the capillary pressure function leads to more reasonable contact angle values. In Section 5 of the paper, we will provide corroboration of computed and experimental results.

4. Experimental measurements

Experimental measurements of a capillary pressure function on sediment cores are based on measurements of the difference in pressure between the nonwetting and wetting phases, both of which are flowing through a porous medium. Experiments are usually conducted under steady-state or transient conditions. Controlling the relative injection rates of the two fluids can set the saturation at which the pressure difference between the nonwetting and wetting phases is measured. Evaluation of the average saturation of the core based on the material balance technique allows one to avoid the use of sophisticated equipment to measure the saturation. In this paper, we present the results of an experiment, which is described in more detail in [1]. Fig. 3 depicts a schematic of the equipment used to measure the capillary pressure between a nonwetting and a wetting fluid flowing through a porous medium. The schematic is a cross-sectional view of the core holder taken orthogonal to the direction of flow. The cross section is located midway along the length of the core. The width of the core holder is 10 cm and the height is 4 cm, while the width of the porous medium is 5 cm and the height is 1 cm. The wall thickness of the core holder depends primarily on the pressures at which the experiment will be run. Note that the wall must be thick enough to accommodate easily the barrel of the pressure transducers. Note also that there are two pressure transducers, one to measure the pressure in the oil and one to measure the pressure in the water. The difference in pressure can be determined using a differential pressure transducer design.

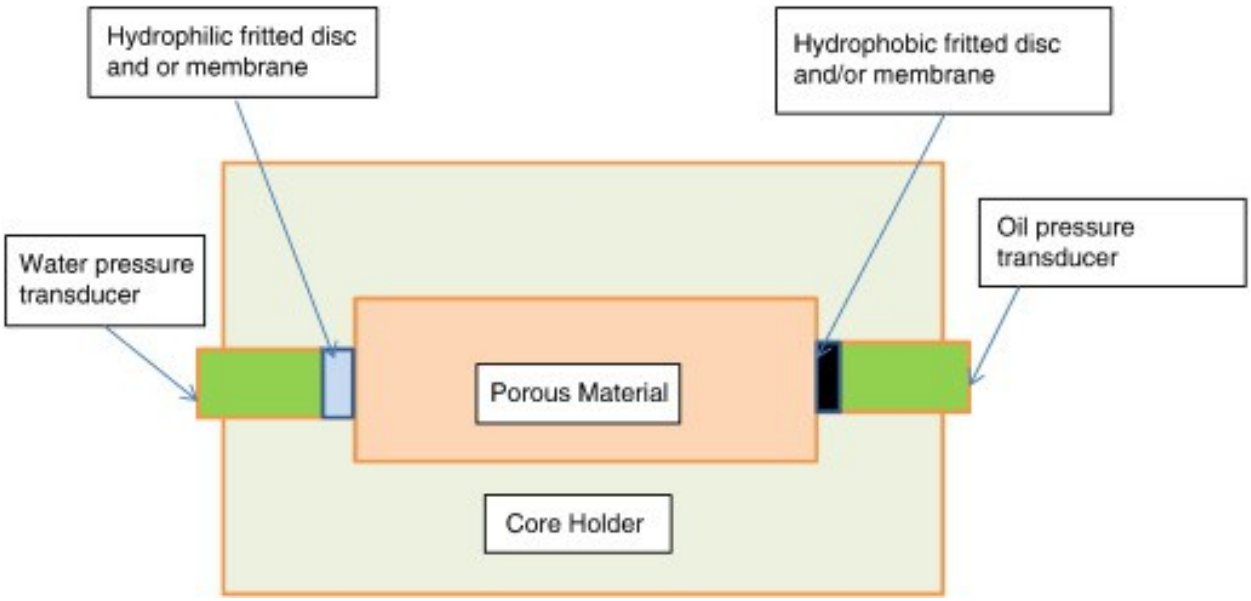

1. Download high-res image (159KB)
2. Download full-size image

Fig. 3. Cross-sectional view of core holder and porous material. After Ayub and Bentsen [11].

The capacitive differential pressure sensor utilized in this study uses the difference between two pressure sources to estimate the pressure. The external pressure (pressure being measured) acts downward on the top membrane (Fig. 4). The pressure cavity (region above the bottom plate in Fig. 4) is filled with the reference pressure (atmospheric), which is confined by the diaphragm (top) membrane. The sensor measures the change in pressure, which comes about because of the downward deflection of the membrane due to the pressure acting downward on the membrane. The diaphragm and pressure cavity create a variable capacitor to detect the strain caused by the applied pressure. As the distance between the diaphragm and the bottom plate decreases, the effective capacitance increases, which can be related to the magnitude of the downward acting pressure.

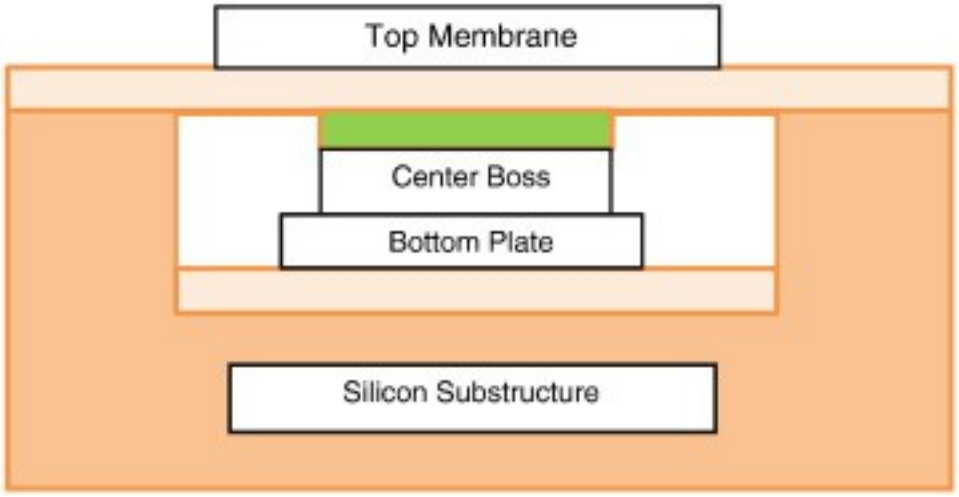

1. Download high-res image (88KB)
2. Download full-size image

Fig. 4. Schematic diagram of bossed diaphragm capacitive pressure sensor. After Ayub and Bentsen [11].

To ensure that the oil transducer measures only the pressure in the oil, and the water pressure transducer measures only the pressure in the water, the pressure in the oil is sensed through a hydrophobic fritted disc, which supports a hydrophobic membrane, and the pressure in the water is sensed through a hydrophilic fritted disc, which supports a hydrophilic membrane. The membranes are placed between the fritted disc and the porous medium so that they are flush with the inner wall of the core holder. The advantage of using a membrane supported on a disc is that this approach enables the design of a system, which not only responds rapidly to changes in pressure but also has a high displacement pressure. This is of particular importance in the design of the system used to measure the pressure in the water. In order to react rapidly to changes in pressure, the hydrophilic fritted disc needs to have a high permeability (porosity). Because, in a water-wet porous medium, the pressure in the oil is always higher than it is in the water, it is highly unlikely that any water will pass through the fritted hydrophobic disc to compromise the accuracy of the oil pressure measurement. Consequently, it is usually not necessary to use a membrane in conjunction with the hydrophobic fritted disc. Strongly hydrophobic Teflon discs (manufactured by KONTES Scientific Glassware/Instrument) were mounted on the fluid intake ports of the pressure transducers to sense the pressures in the oleic phase. No changes in the wetting characteristics of the Teflon discs were observed during the course of a run, a problem encountered when using locally manufactured fritted discs to sense the pressure in the oil.

The situation is more complicated for water pressure measurements because the following two conditions must be met in the system design. First, in order to be able to react rapidly to changes in pressure, the hydrophilic fritted disc must have a high permeability (porosity). Second, in order to prevent oil from passing through the fritted disc and, as a consequence, compromising the accuracy of the pressure measurement, the hydrophilic fritted disc must have a low permeability (porosity), so that it has a high displacement pressure. It is not possible to satisfy both requirements with one material. As a way around this problem, it is suggested that the hydrophilic fritted disc be composed of high permeability (porosity) material, enabling rapid transmission of changes in pressure, while the hydrophilic membrane be composed of low permeability (porosity) material, so that it has a high displacement pressure. Because the membrane is so thin, its low permeability should not distract seriously from its ability to transmit changes in pressure rapidly. After an extended search, it was discovered that the membranes supplied by the Millipore Corporation with minimum protein binding and a high bubble point pressure enabled the most accurate sensing of pressure in the aqueous phase. To provide support for these membranes, fritted discs manufactured by CORNING Corporation were used.

In order that the pressure measured in a given phase, say water, is representative of the pressure across the entire cross-sectional area of the core located between the two pressure transducers, the water flowing across the sensing element of the transducer must be connected to the water flowing through the entire cross section. As the water saturation in the core approaches its irreducible value, S_{wi}, it becomes increasingly unlikely that this requirement is met. Similar comments can be made about the accuracy of the oil pressure measurements as the saturation to oil approaches its residual value, S_{or}. Consequently, the capillary pressure measuring device described herein cannot be used to measure the capillary pressure at the end-point values of saturation, S_{wi} and S_{or}.

The central section of the core holder, where pressures are measured, should be at least 10 cm in length. Moreover, in order to avoid end effects, the core holder should be designed to have an additional length of 10 cm on the inlet end to avoid inlet end effects, and an additional length of 10 cm on the production end to avoid outlet end effects, for a total length of 30 cm. Inlet end effects arise because of local entry of the injected fluids. This problem can be eliminated, or at least ameliorated, by injecting the wetting phase through a hydrophilic fritted plate and by injecting the nonwetting phase through a hydrophobic fritted plate, both of which can be built into the inlet end cap (Fig. 5). The capillarity of the fritted plate causes the injected fluid to spread across the

entire cross-sectional area of the fritted plate, reducing significantly the possibility that local entry of the injected fluid will take place. Outlet end effects arise because of the discontinuity in pressure at the outlet end of the core. Again, this problem can be ameliorated by producing the water through a hydrophilic fritted plate, and by producing the oil through a hydrophobic fritted plate, both of which can be located in the outlet end cap (see Fig. 5). This approach has the added advantage that the material balance calculations needed to estimate the average saturation in the core are simplified because individual measurements of the quantity of each produced phase are available.

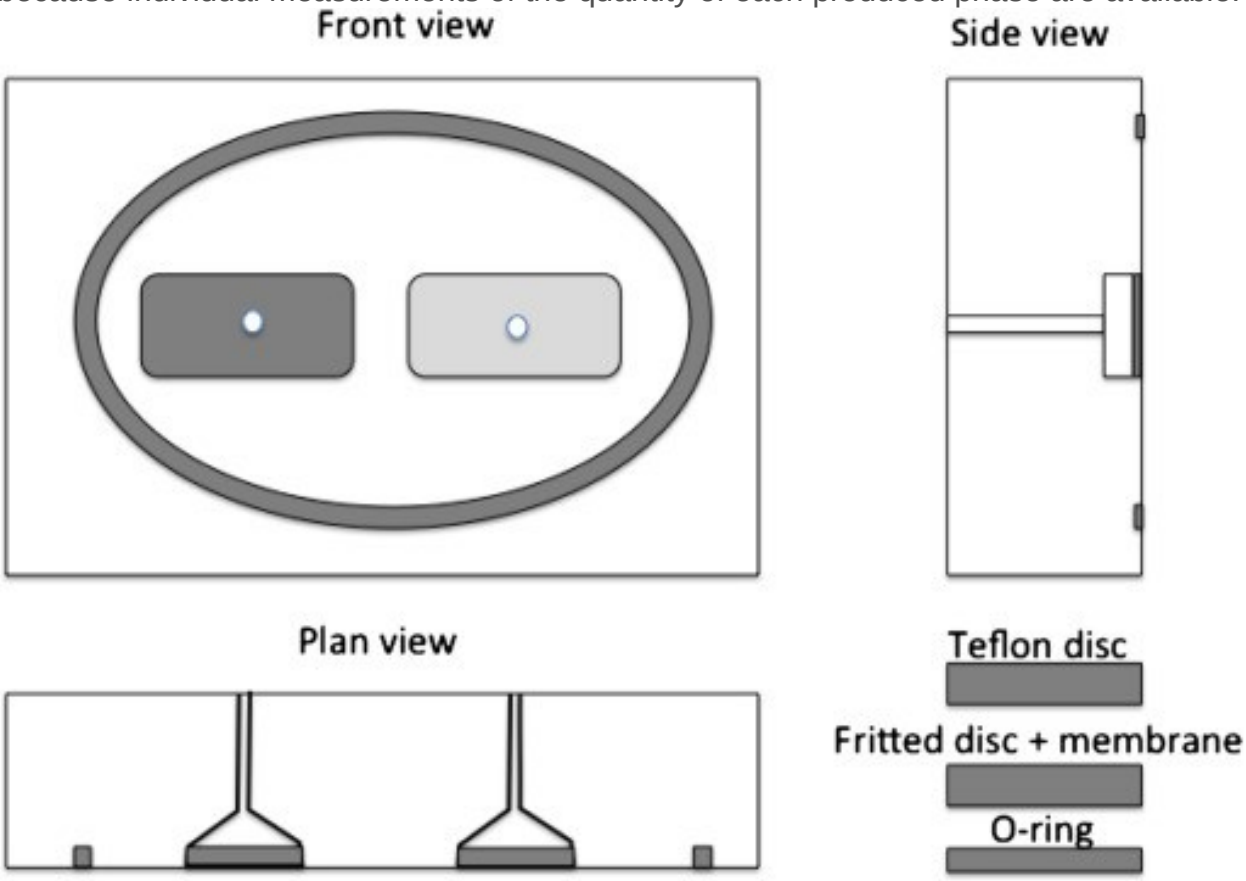

1. Download high-res image (188KB)
2. Download full-size image

Fig. 5. Schematic of the end cap for the core holder (not to scale). After Ayub and Bentsen [11].

The results obtained from this core experiment are available in [11]. The porosityand the permeability of the unconsolidated core used in the experiment are given in Table 1. Water was used as the wetting phase and a kerosene-light mineral oilmixture having a density of 0.83 g/ml and a viscosity of μ = 15 mPa·s was used as the nonwetting fluid. The capillary pressures at the end-point saturations S_{wi} and S_{or} were not measured

directly and were determined by extrapolation of a capillary pressure curve. To evaluate the relative effect of viscous forces versus surface tension acting across an interface between two immiscible liquids, we calculated the nondimensional capillary number (Ca) from the following formula:

$$Ca = \mu V / \gamma_{ow}$$

Table 1. Parameters used for calculations of P_c.

Parameters		Das et al. (2004)	Beckner et al. (1988) (cited in 32, Fig. 9)	Collins (1961, Figs. 6–13)	Ayub and Bentsen (2001)
Porosity, ϕ		0.4	0.25*	0.32	0.373
Permeability, K (m^2)		5.00E − 12	2.90E − 12	1.97E − 13	1.905E − 13
Surface tension, γ_{nw} (N/m)		0.02	0.048	0.048	0.043
S_{rn}		0.92	0.75	0.85	–
S_{rw}		0.098	0.346	0.092	–
A (bars)		0.0135	0.04	0.1	N/A
Calculated apparent contact angle	Using Eq. (11) in Babchin and Faybishenko (2014)	87	80	84	89
Θ (deg)	Single capillaries (using Eq. (30))	79	11	62	82
	Orthogonal capillaries (using Eq. (30))	71	**	37	77
Nonwetting fluid		PCE	Oil	Oil	Kerosene–oil mixture

* ∅ = 0.225 was used in Babchin and Faybishenko (2014).

** Not applicable, because calculated cos (Θ) > 1 (due to low porosity).

Using a viscosity of μ = 15 mP·s, γ_{ow} = 0.043 N/m, and V = 1.86 × 10^{-6} m/s (for the unity gradient and based on the permeability of 1.905E-13 m^2; see Table 1 of the manuscript), we calculated Ca = 1.5 × 10^{-7}, which is considerably less that the Ca number where viscous forces affect the capillary pressure. This calculation proves theoretically that static capillary pressure and dynamic relative permeability functions are compatible.

5. Results of calculations of the capillary pressure function using capillary models

The application of the capillary bundle models was applied (a) to revise the results of calculations of the effective contact angles based on published P_c and relative permeability curves [4], [5], [6] and (b) to validate the application of the capillary bundle models, using the results of the experiment given in Section 4.2. The input parameters for calculations of relative permeability and P_c curves are summarized in Table 1. Table 1 also includes the calculated values of the apparent contact angles, which are, in fact, the fitting parameters needed to match the experimental and calculated P_c curves. (For the graphical presentation of the match between the experimental and calculated P_c curves based on data presented in the literature [4], [5], [6], the reader is referred to Fig. 1, Fig. 2, Fig. 3, Fig. 4 in the paper by Babchin and Faybishenko [3].) Table 1 illustrates that the use of the single and bundle of capillaries model (Eqs. (30) and (31)) reduces the calculated contact angle, which makes the values of the contact angle more realistic.

Fig. 6, Fig. 7, Fig. 8 depict the relative permeability curves, apparent specific areas vs. saturation, and the resulting relationships P_c vs. S_w.

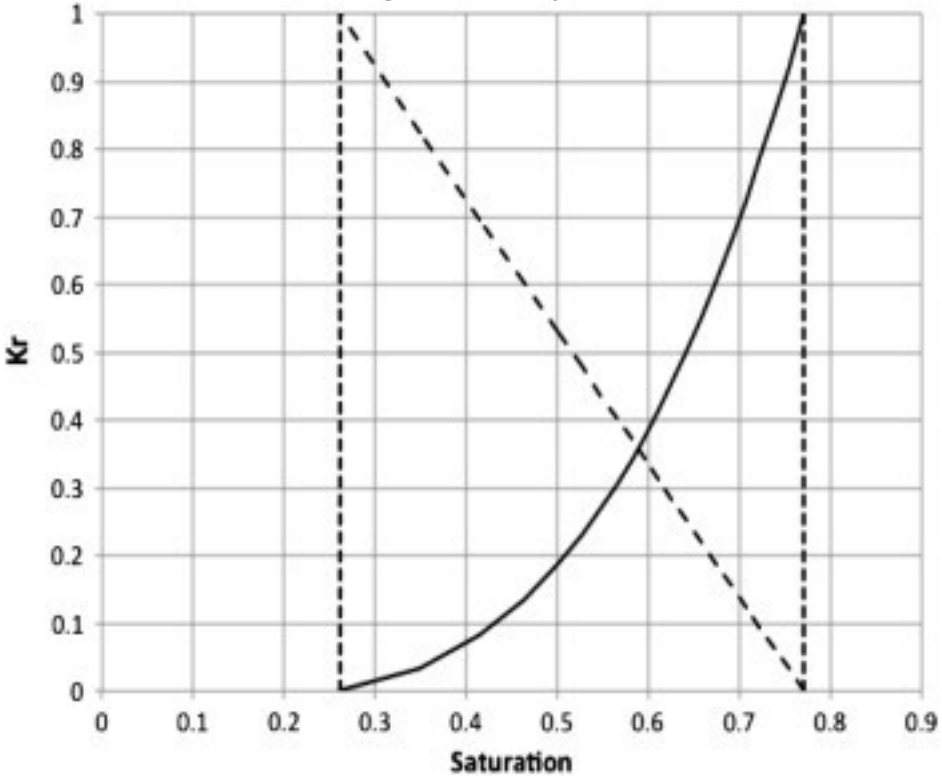

1. Download high-res image (152KB)
2. Download full-size image

Fig. 6. Relative permeability curves for wetting (solid line) and nonwetting (dashed line) phases in the sand sample used in the experiment by Ayub and Bentsen [11]. Vertical dashed lines are residual wetting (left) and nonwetting (right) saturations.

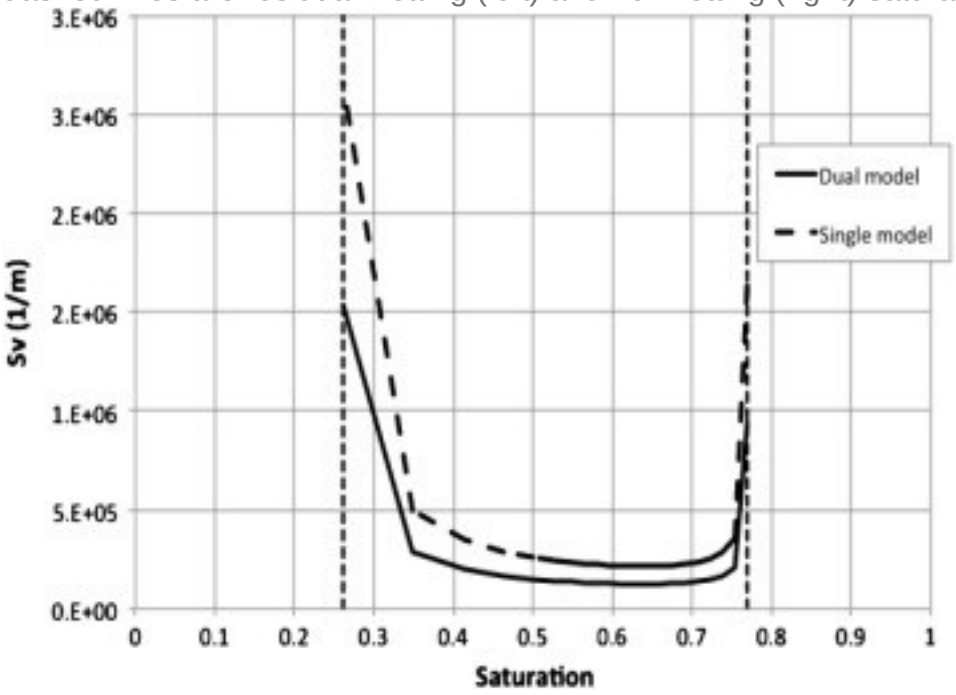

1. Download high-res image (138KB)
2. Download full-size image

Fig. 7. Calculated specific surface area vs. normalized wetting-phase saturation calculated from the experimental data in Ayub and Bentsen [11] for the single and dual bundle capillaries models. Vertical dashed lines are residual wetting (left) and nonwetting (right) saturations.

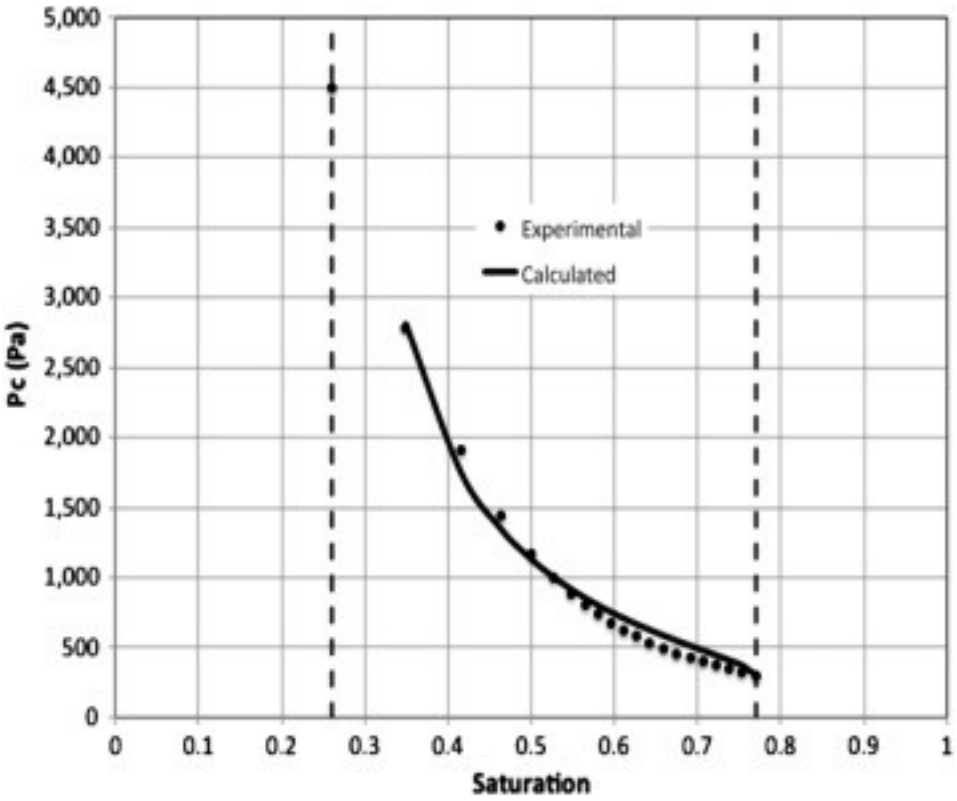

1. Download high-res image (153KB)
2. Download full-size image

Fig. 8. Experimental [11] and calculated P_c curves from Eqs. (33), (34), using the contact angles given in Table 1.

Note that the calculated contact angles $0 < \Theta < 90°$ are indicative of water-wet conditions. The application of the models of the bundle of single capillaries and the bundle of orthogonal capillaries reduce the calculated contact angles. In general, the fact that the calculated contact angles $\Theta > 0$ can be explained by the fractional wettability of porous media [7], [33]. While for all cases, the model given in [3] is applicable, the models of bundles of single capillaries and orthogonal capillaries are not pertinent for some cases. Both models are not applicable for the data from Collins [4], and the model of orthogonal capillaries is not applicable for the data from Beckner et al. [6], as the calculated $\cos \Theta > 1$.

Based on the approach introduced in the paper by Babchin and Faybishenko [3], we can present a general form of the Leverett J_m function given by

(37)Jmsw=PcPc−ASvsnKp

where a new term K_p is expressed depending on the model of S_v:Kp=Kϕ for the model given in Babchin and Faybishenko (2014)

Sv=1/Kp1/Krnw1/2+1/Krw1/2

and Kp=nKϕ31/2,where n = 2 and n = 6 for the models of bundles of singular (Eq. (33)) and orthogonal (Eq. (34)) capillaries.

For the imbibition curve, when A = 0, Eq. (37) can be simplified to

(38)Jmsw=SvsnKp

Babchin and Faybishenko [3, Fig. 5] showed that despite a significant difference in absolute and relative permeabilities and capillary pressure curves, the modified Leverett function (J_m) vs. the normalized wetting saturation (s_w) describes experimental data well. Thus, assuming the same permeability of porous media, the equations for K_p are given by

(a)

In the paper by Babchin and Faybishenko [3]: $K_p = (\phi/k)^{0.5}$

(b)

In this paper, for a single bundle: $K_p = (\phi^3/2\ k)^{0.5}$

(c)

In this paper, for multiple bundles:

(39)Kp=ϕ3/6k0.5

Thus, S_v is getting smaller from (a) to (b) to (c), which means that for a given P_c, cos Θ must get bigger, so Θ must get smaller (Eq. (36), Table 1). Note that the decrease in S_v as more bundles are added is a result of the assumption of using the same ∅ in Table 1 for all three cases. Substitution of Eq. (39), which are different models of the specific surface area, into Eq. (37) reveals that the functional dependence P_c (S_w) is determined by relative permeability functions of the two fluid phases, which, in turn, are dependent on the porous space geometry.

6. Conclusions

In this paper, the authors extended the application of the analytical solution, initially given in Babchin and Faybishenko [3], for the determination of the capillary pressure curve for two immiscible fluids in porous media, using a combination of the relative permeability functions for the wetting and nonwetting phases along with an equation for the apparent specific surface area and an apparent contact angle. In the current paper, the authors presented the analytical solutions for the P_c curve using the two types of capillary bundles. By using relative permeability functions, we automatically take into account the geometry (topology) and the roughness and crevices of the porous medium, as well as obtain singularities at the residual points, which are difficult to obtain experimentally. The capillary bundle models derived in the paper lead to reasonable values of the contact angle. The authors showed that the application of the single and

bundle capillary models leads to a match between the experimental and calculated P_c curves, using the lower values of the apparent contact angles. The results of the experiment conducted by Ayub and Bentsen [11] were used for the validation of the approach based on the application of the single and bundle capillary models.

Acknowledgment

The work of BF was partially supported by the Sustainable Systems Scientific Focus Area (SFA) program at LBNL, supported by the U.S. Department of Energy, Office of Science, Office of Biological and Environmental Research, Subsurface Biogeochemical Research Program, through contract no. DE-AC02-05CH11231between Lawrence Berkeley National Laboratory and the U. S. Department of Energy. The authors are very thankful to Dr. Christine Doughty of LBNL for her careful review and valuable suggestions, and two anonymous reviewers, whose comments helped the authors to improve the manuscript. The authors would like to express their sincere appreciation to Prof. Clayton Radke, one of the leading Chemical Engineers in the US, for his kind invitation to submit the paper to the Special Issue of the ACIS to honor his 70th Birthday.

References

[1]

J. Mason, N. Morrow**Developments in spontaneous imbibition and possibilities for future work**

J Pet Sci Eng, 110 (2013) (2013), pp. 268-293

View Record in Scopus

[2]

R.G. Larson, N.R. Morrow**Effects of Sample Size on Capillary Pressures in Porous Media**

Powder Technol, 30 (1981), pp. 123-138

ArticleDownload PDFView Record in Scopus

[3]

A.J. Babchin, B. Faybishenko**On the capillary pressure function in porous media based on relative permeabilities of two immiscible fluids**

Colloids Surf A Physicochem Eng Asp, 462 (2014), pp. 225-230

ArticleDownload PDFView Record in Scopus

[4]

R.E. Collins**Flow of Fluids through Porous Materials**

Reinhold Publishing Corporation, New York (1961)

[5]

D.B. Das, S.M. Hassanizadeh, B.E. Rotter, B. Ataie-Ashtiani**A numerical study of micro-heterogeneity effects on upscaled properties of two-phase flow in porous media**

Transp Porous Media, 56 (2004), pp. 329-350
CrossRefView Record in Scopus

[6]

B.L. Beckner, A. Firoozabadi, K. Aziz**Modeling transverse imbibition in double-porosity simulators, paper presented at SPE California Regional Meeting, Long Beach, Calif.** (1988)
[23–25 March]

[7]

S.A. Bradford, F.J. Leij**Fractional wettability effects on two-and three-fluid capillary pressure-saturation relations**
J Contam Hydrol, 20 (1995), pp. 89-109
ArticleDownload PDFView Record in Scopus

[8]

H.Sh. Behbahani, M.J. Blunt**Analysis of imbibition in mixed wet rocks using pore-scale modelling**
SPE 90132, Annual Technical Conference and Exhibition, Houston, Texas, USA (2004)

[9]

L.L. Schramm**Surfactants: Fundamentals and Applications in the Petroleum Industry**
Cambridge University Press (2010)

[10]

D.M. O'Carroll, L.M. Abriola, C.A. Polityka, S.A. Bradford, A.H. Demond**Prediction of two-phase capillary pressure–saturation relationships in fractional wettability systems**
J Contam Hydrol, 77 (2005), pp. 247-270
ArticleDownload PDFView Record in Scopus

[11]

M. Ayub, R.G. Bentsen**An apparatus for simultaneous measurement of relative permeability and dynamic capillary pressure**
Pet Sci Technol, vol. 19 (Nos.09-10) (2001), pp. 1129-1154
CrossRefView Record in Scopus

[12]

X.Y. Zhang, R.G. Bentsen, L.B. Cunha**Investigations of Interfacial Coupling Phenomena and its Impact on Recovery Factor**
J Can Pet Technol, 47 (7) (2008), pp. 26-32
View Record in Scopus

[13]

Handbook of HPLC
E. Katz, *et al.* (Eds.), Chromatographic Science, vol. 78, Marcel Dekker, Inc. (1998)

[4]

G.I. Barenblatt, V.M. Entov, V.M. Ryzhik**Theory of Fluid Flows Through Natural Rocks (Theory and Applications of Transport in Porous Media)**
Kluwer Academic Publishers (1990)

[15]

F.A.L. Dullien**Porous Media. Fluid Transport and Porous structure**
Academic Press (1992)

[16]

J. Bear**Dynamics of Fluids in Porous Media**
Dover Publications (1972)

[17]

N.T. Burdine**Relative permeability calculations from pore size distribution data**
Trans AIME, 198 (1953), p. 71
CrossRefView Record in Scopus

[18]

L.A. Rapoport, W.J. Leas**Relative permeability to liquid in liquid-gas systems**
Trans Am Inst Min Metall Pet Eng, 192 (1951), pp. 83-95
View Record in Scopus

[19]

P. Reeves, M. Celia**A functional relationship between capillary pressure, saturation, and interfacial area as revealed by a pore-scale network model**
Water Resour Res, 32 (1996), pp. 2345-2358
CrossRefView Record in Scopus

[20]

P. Held, M. Celia**Modeling support of functional relationships between capillary pressure, saturation, interfacial area and common lines**
Adv Water Resour, 24 (2001), pp. 325-343
View Record in Scopus

[21]

K.A. Culligan, D. Wildenschild, B.S. Christensen, W.G. Gray, M.L. Rivers, A.F.B. Tompson**Interfacial area measurements for unsaturated flow through a porous medium**
Water Resour Res, 40 (2004), p. W12413

[22]

J. Niessner, S.M. Hassanizadeh**A model for two-phase flow in porous media including fluid–fluid interfacial area**
Water Resour Res, 44 (2008), p. W08439

[23]

W.G. Gray, S.M. Hassanizadeh**Averaging theorems and averaged equations for transport of interface properties in multiphase systems**
Int J Multiphase Flow, 15 (1989), pp. 81-95
ArticleDownload PDFView Record in Scopus

[24]

W.G. Gray, A.F.B. Tompson, W.E. Soll**Closure conditions for two-fluid flow in porous media**
Transp Porous Media, 47 (2002), pp. 29-65
View Record in Scopus

[25]

V. Joekar-Niasar, S.M. Hassanizadeh, A. Leijnse**Insights into the relationship among capillary pressure, saturation, interfacial area and relative permeability using pore-scale network modeling**
Transp Porous Media, 74 (2008), pp. 201-219
CrossRefView Record in Scopus

[26]

Babchin, J.-Y. Yuang**On the capillary coupling between two phases in a droplet train model**
Transp Porous Media, 26 (1997), pp. 225-228
View Record in Scopus

[27]

A.J. Babchin, T.N. Nasr**Analytical model of the capillary pressure gradient in oil–water–rock system**
Transp Porous Media, 65 (2006), pp. 359-362
CrossRefView Record in Scopus

[28]

R.H. Brooks, A.T. Corey**Hydraulic properties of porous media**
Hydrol. Pap., 3, Colorado State University, Fort Collins (1964)

[29]

H.B. Bradley**Petroleum Engineering Handbook**
(1st ed), Society of Petroleum Engineers, 1-55563-010-3 (1987)

[30]

N.R. Morrow**A review of the effects of initial saturation, pore structure and wettability on oil recovery by waterflooding**
Proc. North Sea Oil and Gas Reservoirs Seminar, Trondheim, Graham and Trotman, Ltd, London (1987), pp. 179-191
[December 2-4, 1985]

[31]

E.C. Donaldson, G.V. Chilingarian, T.F. Yen**Enhanced Oil Recovery, II: Processes and Operations**
Elsevier (1989)

[32]

K. Li, R.N. Horne**Comparison of methods to calculate relative permeability from capillary pressure in consolidated water-wet porous media**

Water Resour Res, 42 (2005), p. W06405

[33]

L. Boinovich, A.M. Emelyanenko**The analysis of the parameters of three-phase coexistence in the course of long-term contact between a superhydrophobic surface and an aqueous medium**

Chem Lett, 41 (2012)

[34]

J.R. Bartley, D.W. Ruth**Relative permeability analysis of tube bundle models**

Transp Porous Media, vol. 36 (1999), pp. 161-187, 10.1023/A:1006575231732

View Record in Scopus

[35]

J.R. Bartley, D.W. Ruth**Relative permeability analysis of tube bundle models, including capillary pressure**

Transp Porous Media, 45 (1999), pp. 447-480

View Record in Scopus

[36]

J. Wang, M. Dong, J. Yao**Calculation of relative permeability in reservoir engineering using an interacting triangular tube bundle model**

Particuology, 10 (2012), pp. 710-721

ArticleDownload PDFView Record in Scopus

[37]

D.W. Ruth, J.R. Bartley**Capillary tube models with interaction between the tubes**

[A Note on “Immiscible Displacement in the Interacting Capillary Bundle Model Part I. Development of Interacting Capillary Bundle Model”, by Dong, M., Dullien, F.A.L., Dai, L. and Li, D., 2005, Transport Porous Media]

Transp Porous Media, vol. 86 (Issue 2) (January 2011), pp. 479-482

CrossRefView Record in Scopus

[38]

M. Dong, F.A.L. Dullien, L. Dai, D. Li**Immiscible displacement in the interacting capillary bundle model: Part I. Development of interacting capillary bundle model**

Transp Porous Media, 59 (2005), pp. 1-18

CrossRefView Record in Scopus

[39]

H.K. Dahle, M.A. Celia, S.M. Hassanizadeh**Bundle-of-tubes model for calculating dynamic effects in the capillary–pressure–saturation relationship**

Transp Porous Media, 58 (1–2) (2005), pp. 5-22

CrossRefView Record in Scopus

[40]

A. Hunt, R. Ewing, B. Ghanbarian**Percolation Theory for Flow in Porous Media**
Springer (2014)